Cerebral Cortex December 2010;20:2776–2786
doi:10.1093/cercor/bhq024
Advance Access publication March 8, 2010

Specificity of Neuronal Responses in Primary Visual Cortex Is Modulated by Interhemispheric CorticoCortical Input

Kerstin E. Schmidt[1], Stephen G. Lomber[2] and Giorgio M. Innocenti[3]

[1]Max-Planck Research Group: Cortical Function and Dynamics, Max Planck Institute for Brain Research, 60528 Frankfurt/Main, Germany, [2]Centre for Brain and Mind, Department of Physiology and Pharmacology, Schulich School of Medicine and Dentistry, University of Western Ontario, London, Ontario N6A 5C1, Canada and [3]Division of Neuroanatomy and Brain Development, Department of Neuroscience, Karolinska Institute, 171 77 Stockholm, Sweden

Address correspondence to Dr Kerstin E. Schmidt, Max-Planck Research Group: Cortical Function and Dynamics, Max Planck Institute for Brain Research, Deutschordenstraße 46, 60528 Frankfurt/Main, Germany. Email: schmidt@mpih-frankfurt.mpg.de.

Within the visual cortex, it has been proposed that interhemispheric interactions serve to re-establish the continuity of the visual field across its vertical meridian (VM) by mechanisms similar to those used by intrinsic connections within a hemisphere. However, other specific functions of transcallosal projections have also been proposed, including contributing to disparity tuning and depth perception. Here, we consider whether interhemispheric connections modulate specific response properties, orientation and direction selectivity, of neurons in areas 17 and 18 of the ferret by combining reversible thermal deactivation in one hemisphere with optical imaging of intrinsic signals and single-cell electrophysiology in the other hemisphere. We found interhemispheric influences on both the strength and specificity of the responses to stimulus orientation and direction of motion, predominantly at the VM. However, neurons and domains preferring cardinal contours, in particular vertical contours, seem to receive stronger interhemispheric input than others. This finding is compatible with interhemispheric connections being involved in horizontal disparity tuning. In conclusion, our results support the view that interhemispheric interactions mainly perform integrative functions similar to those of connections intrinsic to one hemisphere.

Keywords: cooling deactivation, corpus callosum, ferret, optical imaging, orientation selectivity

Introduction

The visual field is split in 2 halves (hemifields) at its vertical midline. Each hemifield is separately represented in the visual areas of the contralateral hemisphere. In carnivores, a narrow vertical region including the vertical meridian (VM) of the visual field is represented in both hemispheres. This representation is heavily interconnected through the corpus callosum (CC), the largest brain commissure containing about 56 million axons in primates (LaMantia and Rakic 1990) and 32 million axons in the cat (Berbel and Innocenti 1988). Early reports proposed that these connections served to integrate the cortical representations of the 2 visual hemifields (Choudhury et al. 1965; Hubel and Wiesel 1967), thereby re-establishing the continuity of the visual field. Indeed, numerous optic chiasm section studies have confirmed that the input from the contralateral hemisphere matches the ipsilaterally generated responses in terms of retinal position and orientation preference (Berlucchi and Rizzolatti 1968; Lepore and Guillemot 1982; Antonini et al. 1983; Guillemot et al. 1993; Ptito 2003). In ferrets, the callosally interconnected zone extends considerably beyond the 17/18 border (Grigonis et al. 1992; Innocenti et al. 2002). It roughly overlaps with a 10°-wide zone of bilateral representation of the central visual field in the 2 hemispheres (White et al. 1999; Nakamura et al. 2008). In the equivalent region of the cat, neurons can be driven by callosal input from the contralateral hemisphere as well as by retinogeniculate input (Berlucchi and Rizzolatti 1968; Rochefort et al. 2007), and this bilaterally activated region shrinks following cutting the CC (Payne 1994). This does not occur after lesions of contralateral 17/18 region in the ferret (Nakamura et al. 2008).

It has been proposed that callosal connections are critically involved in horizontal disparity tuning (Blakemore 1969; Mitchell and Blakemore 1970). The question still persists whether callosal connections are a special type of connection or are similar to intrinsic connections in the primary visual cortex and/or to connections between different visual areas. The anatomical organization in cats suggests that they have much in common with both types of connections because they exhibit patchy terminal arbores (Houzel et al. 1994) with clusters of neurons sharing similar orientation preferences (Schmidt et al. 1997; Rochefort et al. 2009).

Earlier attempts to reveal the functional nature of the callosal input in more detail by reversible deactivation of the contralateral hemisphere have shown that callosal connections can increase and/or decrease the responses to visual stimuli in the receiving hemisphere, also depending on the layer of the target neurons (Payne et al. 1991; Payne 1994; Makarov et al. 2008). More important, in both animals (Engel et al. 1991; Nowak et al. 1995; Kiper et al. 1999) and man (Knyazeva et al. 1999; Carmeli et al. 2005), the callosal input synchronizes the responses to visual stimuli in the 2 hemispheres. Therefore, callosal input not only contributes to the creation of transhemispheric neuronal assemblies by synchronizing the activity of neurons in the 2 hemispheres but also modulates the synchronization of a distributed neuronal population in the receiving hemisphere (Carmeli et al. 2007).

It is important to note that most of the callosal interaction effects mentioned above are stimulus specific (i.e., cross-oriented stimuli in both hemifields evoke smaller interactions than iso-oriented ones; Carmeli et al. 2007; Makarov et al. 2008), and small flashing stimuli evoke no interactions at all (Makarov et al. 2008). Therefore, it may be that interhemispheric interactions re-establish the continuity of the visual field by selectively modulating the response to specific stimuli, possibly by increasing the saliency of certain stimulus properties.

In the present study, we investigated the functional impact of visual callosal connections with respect to the orientation

and direction selectivity of the interconnected neurons in areas 17 and 18 of the ferret. We found that callosal connections contribute to the strength and specificity of the orientation and directional response in large regions of areas 17 and 18 representing the central visual field. Neurons or neuronal assemblies responding to vertical contours moving across the vertical midline seem to benefit most from the intact callosal connection. This suggests that callosal connections between neurons preferring vertical contours are either stronger or more frequent, which makes them different from other long-range connections between different parts of the visual field. These findings are compatible with callosal connections contributing to the reconstruction of visual stimuli that cross the boundary between the 2 visual hemifields.

Materials and Methods

Preparation

For the present study, 16 ferrets were obtained from an authorized Swedish breeder. Each ferret was initially anesthetized by an intramuscular injection of ketamine hydrochloride (20 mg/kg) and medetomidine hydrochloride (0.3 mg/kg), supplemented with atropine sulfate (0.15 mg/kg). After tracheotomy and cannulation of the femoral vein, anesthesia was maintained by inhalation of N_2O (70%) and O_2 (30%) supplemented with up to 1.8% isoflurane for surgery and 0.8% isoflurane for recording, together with intravenous application of 0.2 mg/kg/h pancuronium bromide for paralysis. For recording, the eyes were fitted with contact lenses and the pupils dilated with topical application of atropine sulfate and neosynephrine. A craniotomy was performed over areas 17, 18, and 19 in each hemisphere leaving the bone above the superior sagittal sinus intact. The 17/18 border was localized in vivo by the reversal of the receptive field progression toward the visual midline by 2–3 electrophysiological penetrations (Supplementary Fig. 1; see also Innocenti et al. 2002). Eight ferrets were used for the optical recording of intrinsic signals. To accomplish this, a titanium chamber with an inner diameter of 15 mm was implanted over the right hemisphere and a cryoloop (7 × 2 mm^2) (Lomber et al. 1999) was positioned onto the border region between areas 17 and 18 in the left hemisphere (Fig. 1). After removal of the dura, the chamber was filled with silicon oil (Boss Products, Elizabethtown, KY) and sealed with a glass cover slip. After correct positioning, the surface cooling loop was covered with agar (4%) and frequently rinsed with isotonic saline throughout the experiment to prevent the cortex underneath from desiccating. The cryoloops were cooled to 2 ± 1.5 °C by pumping chilled methanol through the lumen of the tubing while monitoring the temperature on the loop.

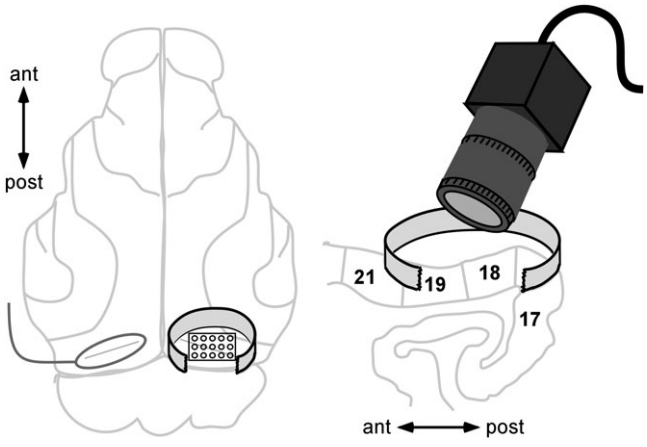

Figure 1. Schematic drawing of experimental setup. The posterior pole of the ferret cortex is exposed on both sides. For electrophysiology, a 15 × 3 matrix is lowered into the 17/18 border region and the recording field covered with agar and bone wax. For optical imaging, a recording chamber is implanted above the superficial parts of areas 17, 18, 19, and 21, sealed with a cover glass and filled with silicon oil. In both experimental parts, a metal cooling loop is positioned on the 17/18 border on the left hemisphere and covered with agar.

In the remaining 8 ferrets, instead of implanting a recording chamber, a 3 × 5 matrix of 410 μm–spaced tungsten microelectrodes (FHC, Bowdoinham, ME) was inserted in the 17/18 border region (Fig. 1) in order to record multiunit activity (MUA) and local field potentials (LFP) from the callosally interconnected cortical region (see also Carmeli et al. 2007; Makarov et al. 2008).

At the conclusion of the experiment, all animals were perfused and their brains prepared for histological processing. The representation of the area 17/18 and the 18/19 borders was identified on Nissl-stained, Gallyas-stained and cytochrome oxidase–stained coronal sections of the occipital pole (Innocenti et al. 2002) and related to the recordings with the help of lesions set after the imaging sessions or by the electrode matrix itself.

Visual Stimulation

Stimuli were presented on a 21″ monitor placed 57 cm in front of the eyes. The monitor was centered between the optical axes of the 2 eyes to optimally stimulate both visual hemifields. In the majority of cases, for accurate positioning of the monitor, the vertical meridian position and its cortical representation were confirmed with single-electrode recordings crossing the 17/18 border in at least 2 sites before and after the imaging or electrophysiological recording session (data not shown), and the eyes were aligned with a prism if necessary. For imaging sessions, 4 whole-field high-contrast gratings were presented. The gratings were held stationary for 500 ms and then moved back and forth orthogonally to their orientation (45° steps) for 3000 ms at a spatial frequency of 0.1 cycle/degree and a speed of 14°/s. For electrophysiological recordings, 8 gratings moving in the 8 different directions (45° steps) were presented at the same spatial frequency and speed.

Optical Imaging of Intrinsic Signals

Five hundred milliseconds after stimulus onset, 5 frames of 600 ms length were recorded with a cooled charge-coupled device camera system (Ora 2001; Optical Imaging Europe, Munich, Germany) under illumination with 605-nm wavelength light for functional images. The field of view was 7.2 × 9.6 mm^2 at a resolution of 192 × 144 pixels and the focus was set 600 μm below the pial surface. Each data set consisted of baseline, cooling, and recovery periods of ~25 min containing 30 repetitions of each of the 4 stimuli. Recording during cooling was initiated 5 min after having reached a stable cryoloop temperature of 2 ± 1.5 °C. Recordings during the recovery period began 20 min after cooling had been discontinued. These temperatures extend deactivating temperatures through all cortical layers and place the critical 20 °C deactivation isotherm at the gray–white matter interface or deeper (Lomber et al. 1999).

For quantitative analysis, optical images were averaged by stimulus condition and filtered by a high pass of 22 pixels and a low pass of 4 pixels. For differential maps, the raw signals evoked by orthogonally oriented gratings were divided by each other. For conventional single-condition maps, a cocktail-blank normalization procedure was applied as well as fixed clipping ranges for baseline, cooling, and recovery sets. Polar maps were computed by vectorially summing up the responses to each stimulus condition and normalizing to the sum vector length, thus providing (for each pixel) a preference angle and a vector strength (VS) value between 0 and 1, for minimal and maximal modulation, respectively. Pixels in up to 3 different regions of interest (ROIs) were analyzed separately. A border ROI was classified as a stripe extending about 0.7 mm into area 17 and 1 mm into area 18 from the 17/18 border previously identified from the electrophysiological and histological data. This corresponds roughly to the region that is callosally interconnected in the ferret (Innocenti et al. 2002). Accordingly, the area 17 and area 18 ROIs were defined by the remaining pixels in the respective area, not belonging to the border region. It is important to note that in addition to the area 17/18 border region ferret area 18 is also densely interconnected by bridges of callosal connections to the contralateral hemisphere (Innocenti et al. 2002).

Electrophysiological Recordings

Recordings targeted the superficial layers of cortex at an estimated depth of 300–800 μm to make the sampling comparable with the optical imaging data. Matrices were positioned in contact with the cortical surface and stabilized with 4% agarose and a bone wax cover before advancing the matrix slowly with an electrically driven micromanipulator (Narishige, Tokyo, Japan). Typically, 3 h elapsed from the time the matrix entered cortex to the first recording. MUA and LFP activity was recorded with a Plexon acquisition system (Plexon Inc., Dallas, TX). MUA was amplified, high pass filtered (100 Hz, 8 kHz), thresholded at 3 standard deviations of the noise level, and time stamps were digitized at 32 kHz. Data sets were kept comparable with the imaging data sets and consisted of 30 repetitions per condition during each of the phases. After the 3500-ms stimulation (500 ms static plus 3000 ms moving), we recorded responses to the iso-luminant screen stimulation for an additional 3000 ms. Units that did not respond significantly higher during stimulation were discarded. In total, 113 neurons from 8 ferrets entered the analysis. Analyses of spike rates were performed for each condition separately in a 2000-ms window starting at 800 ms to prevent the transient response of the stimulus motion onset and to keep the data comparable with the imaging data. Only the 2 responses to the preferred orientation were considered (n = 113 units, 226 responses).

Tuning curves were fitted with a von Mises function as suggested by Swindale (1998) as follows:

$$M(\theta) = A\exp\{\kappa[\cos 2(\theta - \varphi) - 1]\},$$

where, A is the value of the function M at the preferred orientation, φ, θ is the orientation, and κ is a width parameter. From this, orientation tuning bandwidth was extracted as the half-width at half-height of the fitted orientation tuning curve.

Further, orientation selectivity index (OSI) and direction discrimination index (DDI) were computed as discrimination indices for orientation and direction by correcting for the goodness of the tuning fit as suggested by Prince et al. (2002)

$$\mathrm{DDI} = \frac{(\mathrm{Rate}_{\mathrm{preferred}} - \mathrm{Rate}_{\mathrm{null}})}{(\mathrm{Rate}_{\mathrm{preferred}} - \mathrm{Rate}_{\mathrm{null}}) + 2 \times \mathrm{RMSE}},$$

where, RMSE is the square root of the residual variance around the means across the tuning curve.

For evaluation of changes in orientation bandwidth and selectivity changes, only units with a significant fit (r^2 > 0.8; n = 86) were included; for evaluation of changes in direction selectivity only units with a baseline DDI ≥ 0.2 (n = 61) were included.

Results

The Gain of the Population Response at the 17/18 Border Is Modulated by Interhemispheric Input

The first approach used to characterize the influence of interhemispheric connections on the representation of stimuli crossing the vertical meridian was to compute the single-condition maps (Fig. 2) obtained by intrinsic signal imaging. All images recorded for a certain stimulus were averaged for the baseline, cooling, and recovery periods and processed with the same clipping range to maintain comparable gray values in all images. In the baseline maps (Fig. 2*A*, upper row), it is evident that the stimulus activated both areas 17 and 18 (see surface image in Fig. 2*B*) and that maps evoked by cardinal contours exhibited slightly more contrast than maps evoked by oblique contours (Coppola et al. 1998). During cooling deactivation of the topographically corresponding region in the contralateral hemisphere, the contrast in the activity maps decreased markedly, indicating a lower response amplitude (Fig. 2*A*, second row) rebounding to higher than baseline levels during the recovery period (Fig. 2*A*, third row). The contrast change was quantified by computing the normalized VS from the clipped responses to all 4 grating stimuli per baseline, cooling, or recovery period in a compound ROI, including the entire area modulated by the stimulus (Fig. 2*C*). This value indicates the vigor of the response to the preferred orientation per pixel. Cooling decreased the averaged VS. For analysis of the sum data, the stimulated region was split into 3 ROIs (see Materials and Methods section), based on the histological and electrophysiological identification of the 17/18 border (Fig. 2*D*). A clear trend appeared, namely, VS decrease induced by deactivation of interhemispheric inputs affects significantly the border region comprising the callosally interconnected region in areas 17 and 18 (–25.9 ± 15.7%; n = 8; P < 0.05, t-test). However, the effect waned in the more peripheral visual field representations of area 17 (–17.3 ± 7.3%; n = 5; not significant [n.s.]) and area 18 (–14.4 ± 3.7%; n = 5; n.s.).

The Population Response to Vertical Contours Is Selectively Enhanced by Interhemispheric Input

As seen in the single-condition maps of Figure 2*A*, not all orientation responses were equally influenced by deactivating the opposite hemisphere. Modulation by vertical contours (Fig. 2*A*, maps in the first column) attenuated more than modulation by horizontal contours, and the rebound in the recovery was more pronounced. This becomes more apparent in the polar maps that are the result of the pixel-wise vector additions and that display the preference angle per pixel in color and the VS as brightness (Fig. 3*A*). We addressed the issue quantitatively by counting the number of pixels in the border ROI preferring vertical (blue), left oblique (red), horizontal (yellow) and right oblique (green) contours (Fig. 3*B*). Pixels were joined in 4 angle compartments, centered on each of the stimulus orientations and spanning ±22.5° (Fig. 3*B,C*). As expected, for maps of ferret primary visual cortex, the cardinal angles (blue, yellow) predominated over the oblique compartments under baseline conditions (Fig. 3*D*). However, during deactivation of interhemispheric inputs, the number of pixels preferring vertical contours was significantly lower than the number of pixels preferring horizontal contours (Wilcoxon, P < 0.03) and was also lower than the number of pixels preferring oblique contours (Fig. 3*D*). Therefore, responses to vertical contours were selectively weakened, thus leading to a redistribution of pixels to other compartments.

Further analyses were performed to confirm that there was a specific influence of callosal connections on domains responding to vertical contours and that we were not confounded by unequal pixel sample sizes in the 8 different animals. We shifted ROIs of the same size over the border region in one animal and calculated the number of pixels preferring vertical contours during baseline, cooling, and recovery periods (Fig. 4*A*). There was a clear dip in the size of the vertical pixel compartment during cooling over the 17/18 border, which was compensated by an overshooting recovery for that region after rewarming the contralateral hemisphere (Fig. 4*A*). Interestingly, the dip was also observed at the area 19/21 border, which is also densely connected via the CC. The particular example belongs to the rare cases (n = 3) where the respective region had responded to the stimulus.

In addition, we compared the changes in size of the 4 angle compartments in the border and area 18 ROIs (Fig. 4*B*). The shrinkage of the compartment preferring vertical contours at the expense of the other angles was significant. For the area 18 ROI, changes were smaller and more uniform with respect to the different angles (Fig. 4*B*).

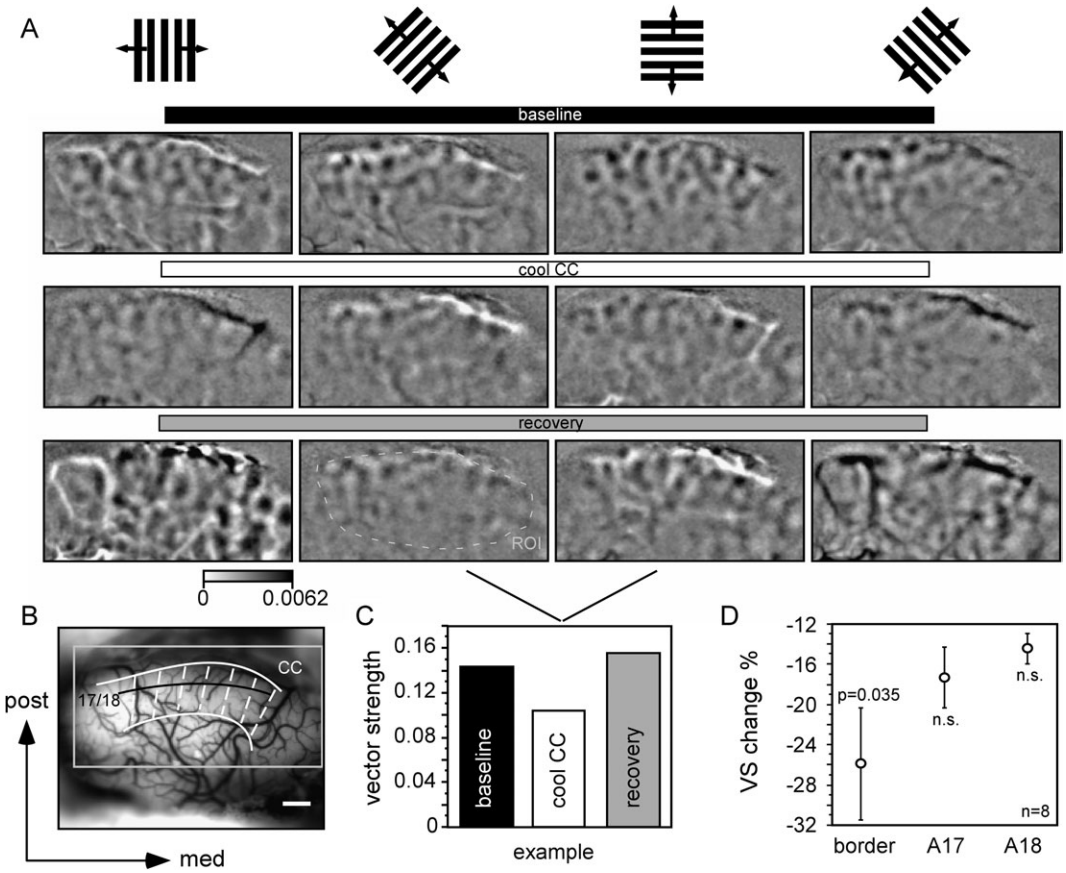

Figure 2. (*A*) Single-condition maps from the right visual cortex obtained with gratings (stimulus sketches above the images apply to one entire column) and intrinsic signal imaging during thermal deactivation of the left visual cortex (cool CC; middle row), baseline (upper row) and rewarming conditions (lower row). Images are cocktail-blank normalized and processed by fixed clipping. Continuation from low (white) to high (black) light absorption is proportional to activation as indicated by the color bar. (*B*) Video image of the entire imaged cortex region with histologically and electrophysiologically confirmed area border in the left hemisphere. The area indicated with white dashed lines is densely interconnected to the other hemisphere by callosal axons. Post, posterior; med, medial; scale bar = 1 mm. (*C*) Average VS in the ROI marked in the last row of (*A*). (*D*) Average VS changes in 8 ferrets during cooling deactivation of the left visual cortex in 3 separated ROIs. The ROI "border" refers to the callosally connected region (dashed in *B*). For the border ROI, there is a significant VS decrease.

The computation of preference angles and VS involves many preprocessing steps like clipping and normalization to a cocktail blank. However, the cooling inactivation also induced an unspecific loss in signal dynamics that might lead to an overestimation of effects on preference angles. Thus, we also compared the raw response profiles obtained by dividing maps obtained by orthogonal contour stimulation with each other. Raw responses obtained by stimulation with vertical (or left oblique) contours were divided by raw responses evoked by horizontal (or right oblique) contours resulting in values distributed between –1 and 1 (Fig. 5*A,B*). All raw responses decreased significantly during cooling deactivation of interhemispheric inputs; however, the vertical angle compartment showed the greatest decrease (Fig. 5*C*).

Responses to the Horizontal Direction of Movement Are Differently Modulated by Callosal Input Than Other Responses

In contrast to our imaging results, previous single-cell studies in cats had shown a rather nonuniform picture of interhemispheric influences on neuronal responses (Payne et al. 1991; Payne 1994). To hopefully resolve this disparity, we compared our imaging results with electrophysiological data obtained in ferrets by applying the same deactivation protocols used for the imaging. Firing rates were significantly changed during cooling ($P < 0.0001$; Wilcoxon signed rank), also in each of the 4 angle compartments separately. In our data from 113 units, we identified a variety of firing increases and decreases during cooling (Fig. 6*A*), albeit with a slight prevalence for the latter in all orientation compartments (Fig. 6*B*). Therefore, qualitative observations of the neuronal recordings seemed to resemble those made by earlier investigations (Payne et al. 1991; Payne 1994). However, a quantitative analysis revealed more specific changes that were consistent with the imaging results (Fig. 6*C,D*). We restricted the analysis to the 2 best responses, the 2 directions in the preferred axis of orientation (n = 226 responses of 113 neurons). In total, 68% of the stimulus-induced firing rates decreased while 32% of responses increased (Fig. 6*A*). We calculated a modulation ratio for comparison of baseline and cooling responses as follows:

$$\text{Rate modulation ratio}_{\text{pre-cool}} = (\text{Response}_{\text{pre}} - \text{Response}_{\text{cool}}) / (\text{Response}_{\text{pre}} + \text{Response}_{\text{cool}}).$$

Statistical analysis of the absolute modulation ratios (mean 0.126 ± 0.126) revealed that units responding to cardinal stimuli

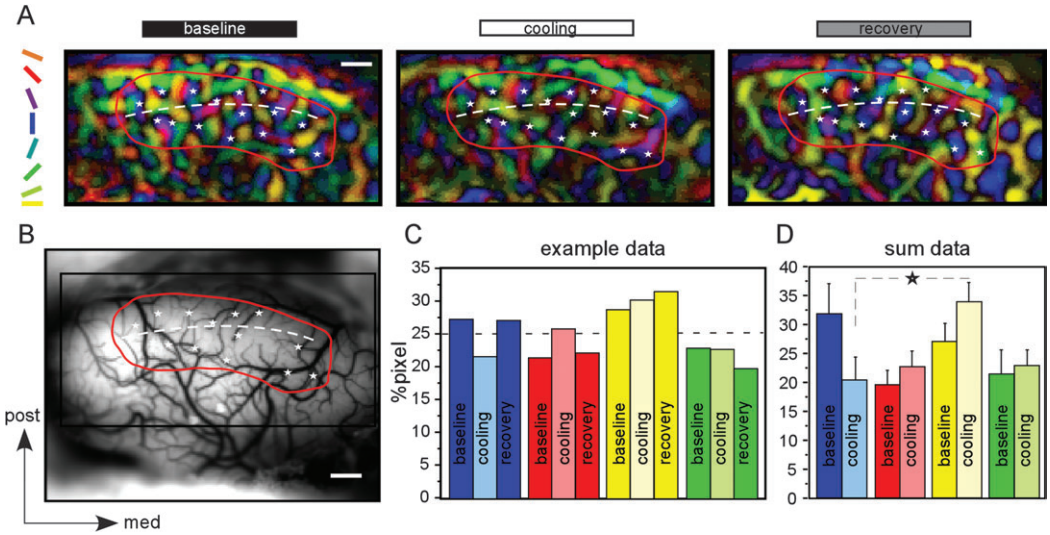

Figure 3. Orientation map changes during thermal deactivation of the left visual cortex. (*A*) Polar maps of the example depicted in Figure 2. In these compound maps, color codes for the orientation preference angle and brightness for the VS per pixel after vector summation of the 4 single-condition maps. White stars are positioned in blue domains that prefer vertical gratings within the baseline map. Note that especially close to the 17/18 border (white dashed line), the blue area beneath the stars shrinks during cooling. (*B*) Vessel picture of the imaged region with landmarks as in Figure 2. The region outlined in red was used for the computations in (*C*). (*C*) Orientation preference distribution of the pixels in the example shown in (*A*); ROI split into 4 compartments, each spanning ±22.5° centered on 45°, 90°, 135°, and 180° orientations. (*D*) Average orientation preference distribution of the pixel distributions in 8 ferrets (border ROIs) during baseline and cooling condition. Observe the known tendency of a higher percentage of cardinally preferring pixels in the baseline maps in (*C*) and (*D*). However, the proportion of vertically preferring pixels decreases at the advantage of the other angle compartments leading to a significant size difference (Wilcoxon) between vertical and horizontal angle compartment during CC cooling.

showed significantly larger changes in either direction than units responding best to oblique stimuli (127 cardinal vs. 99 oblique responses, Mann–Whitney, $P < 0.02$). This holds also true when considering only rate changes significantly larger than the inter-trial variability ($n = 159$ with modulation ratio$_{pre\text{-}cool} \geq 0.05$, Mann–Whitney $P < 0.0001$, 88 cardinal vs. 71 oblique responses, compare Fig. 6*C*). In accordance with the imaging results, absolute modulation ratio changes were largest for neurons responding to horizontal movements and vertical contours (Fig. 6*C*, Mann–Whitney $P < 0.03$, 50 vertical vs. 109 other responses).

By investigating the significant (≥0.05) increases and decreases separately (Fig. 6*D*), it turned out that increases for the vertically tuned neurons are almost as large as decreases. Thus, in particular, the rate increases were significantly larger for vertically tuned than for neurons responding to other contours ($P < 0.003$; Mann–Whitney, 18 vertical vs. 27 other increased responses).

Therefore, we examined possible changes in orientation bandwidth and orientation and direction selectivity. This could be done in units with good tuning fits ($r^2 > 0.8$; $n = 73$). On the grand average, bandwidth did not change significantly (mean –0.03° ± 14.3°, paired *t*-test $P > 0.5$) because both large increases as well as decreases occurred. Only when separating the 4 different orientation compartments and increases from decreases, some specific influences became obvious. As bandwidth is not normalized, we calculated also a

$$\text{Bandwidth modulation ratio}_{pre-cool} = (\text{Bandwidth}_{pre} - \text{Bandwidth}_{cool}) / (\text{Bandwidth}_{pre} + \text{Bandwidth}_{cool}).$$

Accordingly, bandwidth decreases were more frequent for cardinally (67%) as opposed to obliquely tuned neurons (39%), the latter rather increasing their bandwidth (Fig. 7*A*). For 38 cardinally tuned neurons, average bandwidth decreased weakly significantly as opposed to 35 obliquely tuned units (Fig. 7*B*, $P < 0.04$, Mann–Whitney). The few bandwidth increases for neurons tuned to vertical contours were weakly significantly larger than other bandwidth increases (Fig. 7*C*, $P < 0.05$, Mann–Whitney, 5 vertically tuned vs. 30 tuned to other orientations).

The average effect on OSIs was a slight but significant decrease (paired *t*-test $P < 0.05$, mean –0.025 ± 0.11). Here, decreases dominated for cardinally tuned units (62.5%) as opposed to obliquely tuned units (48.7%) (Fig. 7*D*). Among the group of neurons with significant response ratio changes (≥0.05), absolute OSI changes were again largest for vertically tuned neurons (Mann–Whitney $P < 0.05$, 10 vertical vs. 24 other responses).

Changes in the direction discrimination index (DDI; see Materials and Methods) were quantified for units with a baseline index of at least 0.2 and significant response ratio changes (≥0.05) during cooling ($n = 48$). As for the other parameters of the tuning curve, decreases were mainly observed for neurons with cardinal orientation tuning (Fig. 7G, 63.5% decreases for cardinals and only 38.5% decreases for obliques). However, large increases also occurred and thus, the absolute changes are significantly stronger for cardinally than for obliquely tuned neurons ($P < 0.05$, Mann–Whitney, 31 cardinally vs. 17 obliquely tuned units). Similar to orientation bandwidth, DDI increases were larger, but not significantly, for neurons tuned to vertical contours (horizontal movements) than to other contours (Fig. 7*H*).

Discussion

Our results demonstrate a direct contribution of interhemispheric connections to both the strength and specificity of the

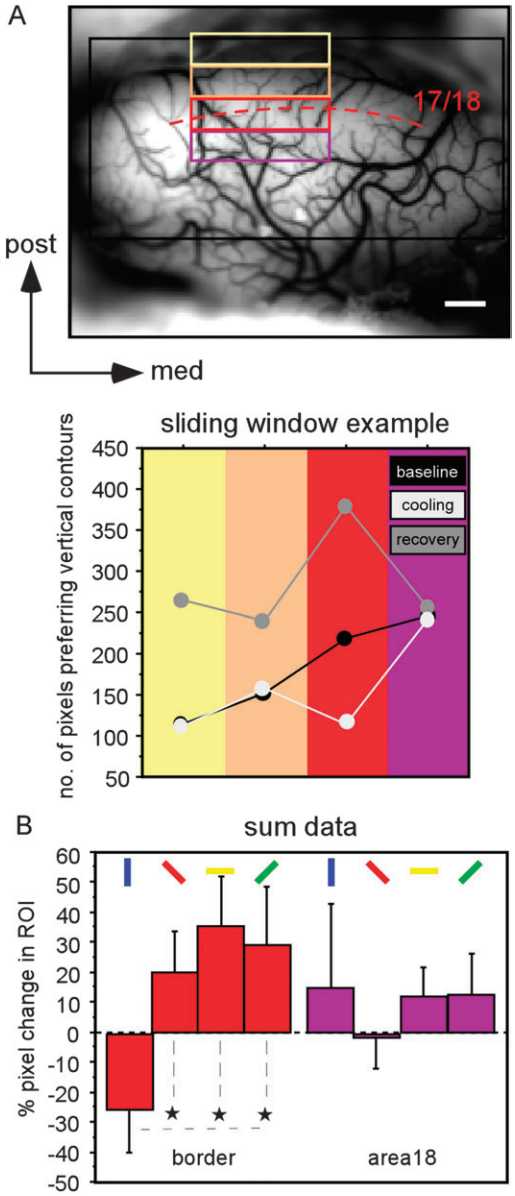

Figure 4. (*A*) Changes in the number of pixels preferring vertical gratings in sliding ROIs of the same size (3.25 × 0.75 mm^2) during baseline, cooling, and recovery conditions. Cortical landmarks as in Figure 2. Note the profound decrease during cooling, accompanied by rebound in recovery, in the red window placed over the 17/18 border. (*B*) Percentage change of the number of pixels in border and area 18 ROIs averaged over all data sets. For the border ROI, the changes in the compartment preferring vertical gratings are significantly different from the changes in the other 3 angle compartments.

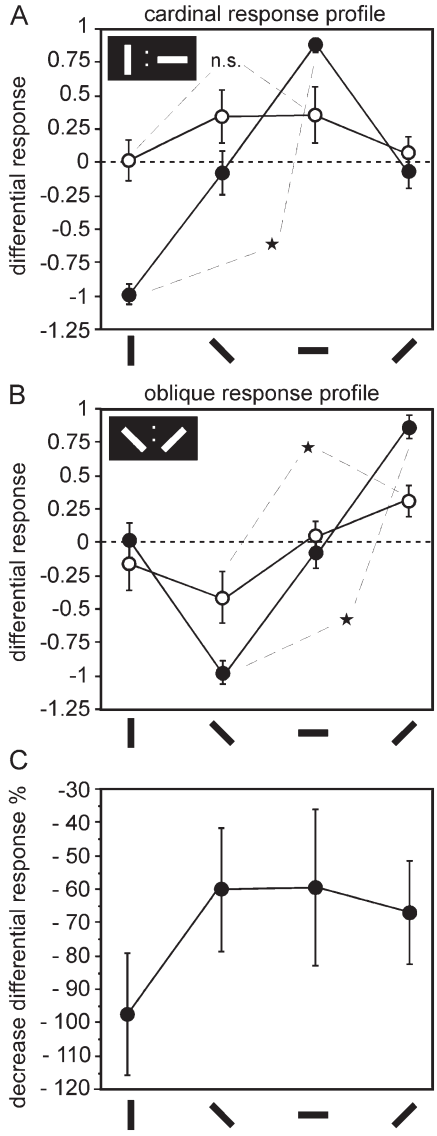

Figure 5. Response profiles for differential maps in 17/18 border ROIs. (*A*) Raw activity distributions obtained with vertical gratings divided by activity distributions obtained with horizontal gratings during baseline (filled circles) and cooling conditions (open circles). Values are averaged over all pixels per angle compartment. (*B*) Raw activity distributions obtained with left oblique gratings divided by activity distributions obtained with right oblique gratings. (*C*) Percentage decrease in absolute response for cardinal (response taken from *A*) and oblique differential responses (values taken from *B*). Note that all responses decrease, but the decrease for the vertical compartment is more profound. As a result, in (*A*), the significant amplitude difference between the 2 cardinal responses in the baseline gets eliminated during cooling whereas oblique responses remain significantly different also during cooling (*B*).

responses to stimulus orientation and direction of motion, predominantly in the zone between areas 17 and 18 in the ferret. This zone receives strong callosal input; removing this input degrades the differential imaging of the responses to gratings covering both visual hemifields. At the electrophysiological level, the loss of callosal input increases or decreases the firing rates and direction selectivity of single units, but deterioration of responses predominates. Together, optical and electrophysiological data demonstrate that single neurons and neuronal domains preferring cardinal contours, in particular vertical contours moving horizontally over the midline, receive stronger callosal input than those activated by other orientations and stimulus motions.

Callosal Connections Modulate Responses Elicited by Thalamocortical Input

In cats, connections via the CC to the contralateral cortex arise mainly from pyramidal and spiny stellate cells, using excitatory amino acids as neurotransmitters (reviewed in Innocenti 1986; Conti and Manzoni 1994). Thus, direct excitatory input to postsynaptic target cells is most likely dominant but not necessarily exclusive since a small population of inhibitory

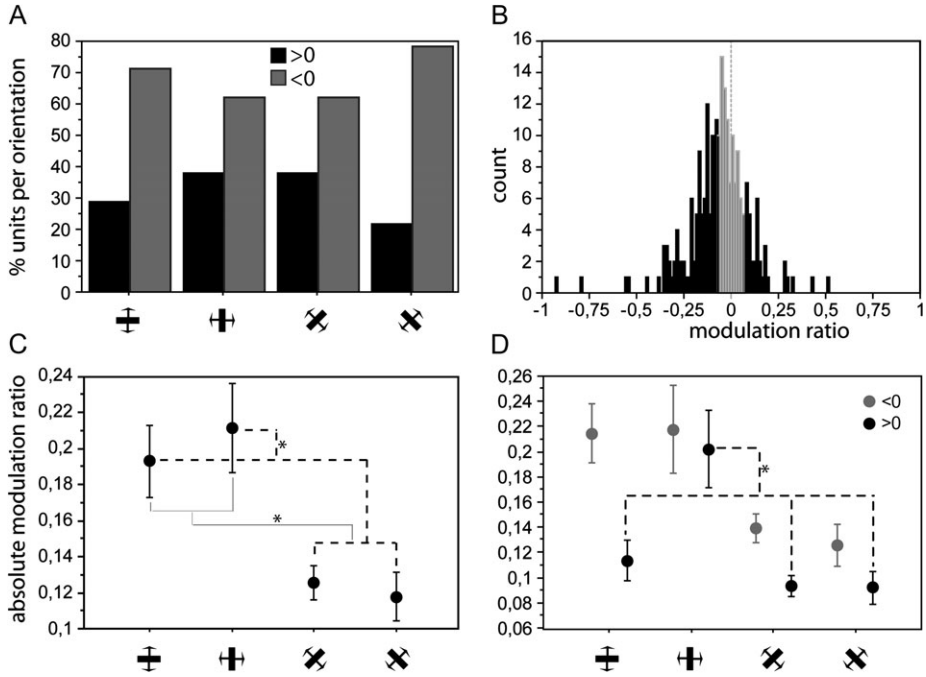

Figure 6. Firing rate changes in electrophysiological unit data ($n = 113$ units) during thermal deactivation of CC. Responses are separated according to stimulus orientation (±22.5°) as indicated by the bar symbols below (*A*, *C*, *D*). As indicated: decreases, filled gray; increases, filled black. (*A*) Distribution of increases and decreases (%) for preferred and least-preferred directions of movement ($n = 226$). Decreases dominate for all angles. (*B*) Histogram of the rate modulation ratios (mean of the decreases -0.14 ± 0.136, mean of the increases 0.095 ± 0.098). For further analysis, only cases with absolute modulation ratio larger than 0.05 (excluding the gray window, $n = 159$) were considered. (*C*) Absolute (both increases and decreases) rate modulation ratio. Note that absolute changes are significantly larger for units preferring cardinal contours and for especially those preferring vertical contours. (*D*) The reason is that for vertically tuned neurons, both increased and decreased responses occur. Stars indicate significant differences (tested with Mann–Whitney).

neurons also projects across the CC (Buhl and Singer 1989; Peters et al. 1990; Hughes and Peters 1992; Fabri and Manzoni 1996). Furthermore, callosal axons can elicit inhibition by contacting inhibitory interneurons (reviewed in Innocenti 1986). Indeed, lesion or inactivation of the CC, or the contralateral hemisphere, causes both increases and decreases in neuronal responses (Payne et al. 1991; Payne 1994; Makarov et al. 2008). Inhibitory effects seem to predominate at shorter latencies, possibly because they are driven by faster-conducting axons (Makarov et al. 2008).

It should be noted that eliminating callosal input to primary visual areas does not eliminate responses to visual stimuli, suggesting that the callosal input has a modulatory, rather than strongly excitatory, effect. This modulatory, rather than driving, role can also be inferred by the morphology of single callosal axons, compared with that of the strongly excitatory thalamocortical axons (Tettoni et al. 1998). It is consistent with the modest size of most of the excitatory postsynaptic potentials elicited by transcallosal stimuli in somatosensory, visual, and association areas of the cat (Innocenti et al. 1972; Toyama et al. 1974; Cissé et al. 2003). One aspect of the modulatory role of callosal input is expressed as synchronization of the neuronal responses in the 2 hemispheres in animals (Engel et al. 1991; Nowak et al. 1995; Kiper et al. 1999) and probably in man (Knyazeva et al. 1999; Carmeli et al. 2005) but also as synchronization or desynchronization of the neuronal responses in the target hemisphere (Carmeli et al. 2007).

The modulatory role of the callosal input between homologous areas seems therefore to be definitely established, and it may be a general feature of callosal connectivity, at least in primary areas. Indeed, it also applies to the somatosensory areas in cats, humans, and rodents (Innocenti et al. 1973; Fabri et al. 2006; Li and Ebner 2006). In the motor cortex, callosal input contributes to the activation of the ipsilateral muscles but only by potentiating the corticofugal projections of the contralateral motor cortex (Brus-Ramer et al. 2009). This somewhat subordinate role of callosal connections is in agreement with the data showing that they require thalamocortical input, driven by visual experience, for their development (reviewed in Innocenti and Price 2005). It should be added that the primary visual areas also receive callosal input from nonprimary visual areas, in particular areas 19, 21, and the suprasylvian complex (Segraves and Rosenquist 1982; Segraves and Innocenti 1985). The present data do not allow inferences on the role of these heterotopic inputs on areas 17 and 18 nor can they be safely generalized to callosal connections in extrastriate visual areas where they seem to contribute to a substantial part of the receptive fields (Gross et al. 1977; Marzi et al. 1982).

It could be argued that callosal input only contributes to a nonspecific increase in the excitability of neurons in areas 17 and 18. This is ruled out by 2 lines of evidence. First, the effects are strongest for neurons and neuronal domains responsive to cardinal stimuli, in particular the vertically oriented stimuli; and second, when stimulating the hemifield contralateral to the recording (the noncooled hemifield), the cooling effects are negligible. These findings unequivocally demonstrate that the callosal input contributes to enhancing the detection of specific aspects of the visual input by activating a specific transhemispheric neuronal assembly.

Transhemispheric Neuronal Assemblies

On the basis of the present and previous results, several properties of the transhemispheric neuronal assemblies

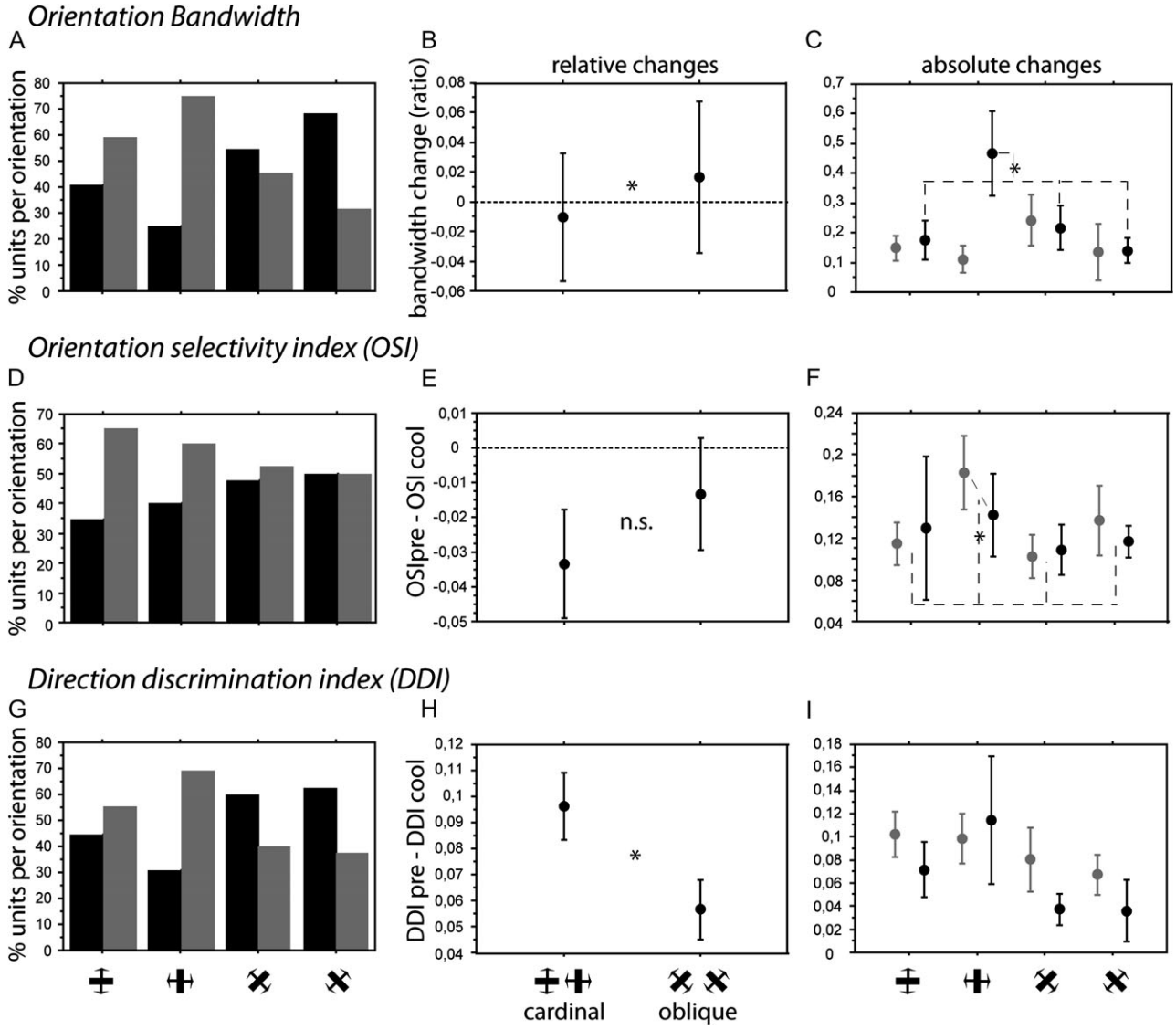

Figure 7. Changes in orientation bandwidth (*A–C*), orientation selectivity (*D–F*), and direction discrimination indices (*G–I*). As indicated: decreases, filled gray; increases, filled black. (*A*, *D*, *G*) The number of decreases (%) is higher for neurons responding to cardinal contours than for neurons responding to oblique contours. (*B*) Accordingly, on average, orientation bandwidth decreases weakly significantly more for cardinal contours. (*C*) In the subset of vertically tuned neurons (5 increases vs. 9 decreases), bandwidth increases are weakly significantly larger than for neurons of other orientation preference. (*E*) The difference between cardinally and obliquely tuned neurons is not significant for changes in orientation selectivity. (*F*) However, absolute OSI changes are significantly larger for neurons preferring vertical contours (horizontal movements) than for other neurons. (*H*) Absolute changes in the DDI are significantly larger for cardinally than for obliquely tuned neurons. (*I*) Separation by orientation reveals elevated (but not significant) increases for vertically tuned neurons.

generated by callosal connections can be specified. First, anatomical evidence indicates that each callosal axon diverges to clusters of terminals corresponding to domains of iso-oriented neurons (Houzel et al. 1994; Schmidt et al. 1997; Rochefort et al. 2009). This has been confirmed by functional evidence (Berlucchi and Rizzolatti 1968; Engel et al. 1991; Rochefort et al. 2007). Second, activation of the interhemispheric assembly requires the use of moving oriented stimuli. No effect of cooling was observed on receptive fields mapped with discrete flashing stimuli (Makarov et al. 2008). Third, as shown in this study, callosal input substantially contributes to the specificity of both orientation and direction responses. This effect is stronger in optical imaging than in electrophysiological data. The enhanced specificity of the responses may be a sharpening effect due to the combined result of the facilitative and suppressive action of callosal input on the single-cell level. The intrinsic signal has the advantage that it provides a comprehensive steady-state picture of a large surface area. The underlying neuronal processes are thought to consist of a mixture of spiking and subthreshold membrane activity, but its exact source is still unclear. Metabolic changes only indirectly relate to the neuronal signals that may also play a role. Thus, removing specific excitatory and inhibitory inputs might disturb coordinated activity patterns, and the network effect will be a lesser modulated orientation map. This interpretation is also supported by the finding that, in split-chiasm cats, a weaker but specific orientation map can be evoked through the contralateral eye by transcallosal input (Rochefort et al. 2007). Fourth, the visual stimulus generates a kind of oscillatory resonance between iso-oriented neurons of the 2 hemispheres (Engel et al. 1991;

Nowak et al. 1995; Kiper et al. 1999; Knyazeva et al. 1999; Carmeli et al. 2005). How this resonance effect and the sharpening of the responses contribute to each other remains to be determined.

Callosal Connections between Homologous Areas Functionally Resemble Local Areal Connections, but. . . .

The leading hypothesis on the nature of callosal connections is that they replicate general features of corticocortical connections, including intra-areal ones, albeit for the restricted portion of the visual field straddling the vertical meridian (Hubel and Wiesel 1967; Innocenti 1986; Kennedy et al. 1991). This is an important hypothesis because it implies that general features of corticocortical connectivity can be studied. This model system has several advantages, including the absence of diverging thalamocortical axons and the possibility of interrupting or inactivating connections with minimal or no interference with other neuronal systems both in maturity and during development. A crucial test of this hypothesis is now possible, by comparing the results of our inactivation of contralateral areas 17 and 18 with those obtained with the local inactivation of local connections in these same primary visual areas. Crook and Eysel (1992) reported broadening of orientation tuning curves in 65% of neurons recorded in area 18 of the cat with the inactivation of local connections between columns of orthogonal orientation. Large broadening of the orientation tuning was occasionally observed in our electrophysiological data especially for vertically tuned neurons, and it might be responsible, in part, for the blurring of imaged orientation domains in our work.

In addition, we observe significant changes in orientation selectivity (Fig. 7*F*) in both our electrophysiological and our optical findings, such as that observed in area 17 of the cat after inactivation of local connections (Girardin and Martin 2009).

Crook et al. (1996) also reported changes in directional preference after inactivation of local connections in area 18, due either to increased response in nonpreferred direction or to decreased response in the preferred direction. We observed similar effects in our electrophysiological recordings (Fig. 7*I*). As for local connections, they can be explained either by the combined loss of excitatory connections between neurons with identical directional preference or by the loss of inhibitory connections between neurons of opposite directional selectivity.

Interestingly, rate changes caused by deactivating the contralateral visual areas affect the cardinal and in particular the vertical orientation system more strongly. The same asymmetry is also expressed in the optically imaged orientation maps. Matching the well-described psychophysical "cardinal effect"—a higher visual acuity for cardinal contours than for oblique contours—a predominance of cells preferring stripes of cardinal orientations in the central visual field has been described for both cats (Pettigrew et al. 1968; Orban and Kennedy 1981; Payne and Berman 1983) and macaque monkeys (Mansfield 1974). A larger cortical area devoted to the representation of cardinal orientations has also been observed in ferrets (Coppola et al. 1998) and cats (Wang et al. 2003). We confirmed that trend in most of our baseline data. Although responses to cardinal contours are usually more vigorous, neurons preferring cardinal contours suffer more from the lack of interhemispheric input than neurons preferring oblique contours. Such asymmetries have not been observed for intrinsic connections, but the possibility—though unlikely—cannot be completely ruled out as the studies investigating the nature of intrinsic connections (for review, Schmidt and Löwel 2002) were not designed to answer that question.

We observe significantly larger rate changes—in particular increases—for neurons tuned to vertical contours and thus to horizontal movement crossing the VM. This may suggest the existence of a strong excitatory and inhibitory network across the CC for this particular subset of neurons in contrast to weaker and predominantly excitatory interactions for neurons preferring other orientations. It is possible that this asymmetry is specific for callosal connections, but it remains to be investigated further. In the densely interconnected central visual field, in particular, binocular simple I and complex cells prefer vertical orientations (Payne and Berman 1983). Thus, these neurons are optimally suited to react to small differences in the horizontal position from both eyes, that is, interocular position disparities. Horizontal disparity is the fundamental cue for depth used in stereopsis (Blakemore 1969). In fact, depth perception in the central visual field is impaired when following CC transaction (Mitchell and Blakemore 1970) but not midsagittal section of the optic chiasm (Blakemore 1970). Following chiasm section, binocularly driven units are still present, thus indicating that the missing input is delivered by interhemispheric connections (Berlucchi and Rizzolatti 1968). Indeed, there is evidence that impairing callosal input diminishes the number of binocular units (Dreher and Cottee 1975; Payne et al. 1980; Blakemore et al. 1983) and the degree of disparity selectivity (Gardner and Cynader 1987). Ferrets exhibit a high number of disparity-selective neurons. Although 20% of all primary visual neurons are driven only by the contralateral eye (Kalberlah et al. 2009), the cortex region we investigated contains the binocular portion of the visual field and ocular dominance columns (Law et al. 1988; White et al. 1999). In this region, 50–60% of the vertically or near vertically driven neurons are modulated by horizontal disparity (Kalberlah et al. 2009). It is thus possible that our results reflect a specific influence of callosal connectivity on horizontal disparity–selective neurons and thus on depth perception.

In conclusion, our results support the view that callosal connections integrate the cortical representation of the 2 hemifields by performing operations similar to those performed by local cortical connections in each hemisphere. In both cases, the role of connections between cortical neurons is that of increasing the salience of certain stimulus parameters, specifically orientation or direction of movement. This computational operation may be a critical component in figure/ground segmentation in vision, which is impaired by lesions of primary visual areas (Kiper et al. 2002). In addition, callosal connections may have a specialized role in mediating information transfer between the central visual field representations of the 2 eyes and may mediate horizontal disparity across the vertical meridian. Our results in the ferret suggest that new tasks testing figure completion across the vertical meridian in normal individuals and in split-brain patients, capturing the specificity of interhemispheric interactions between orientation and direction detectors of the 2 hemispheres, should be designed.

Supplementary Material

Supplementary material can be found at: http://www.cercor.oxfordjournals.org/.

Funding

Max Planck Society to K.E.S.; European Community research contract APEREST to G.M.I.; Swedish Research Council contract (K2002-33X-12594-05B to G.M.I.); Natural Sciences and Engineering Research Council of Canada to S.G.L.

Notes

We are very grateful to Dr Laura Lopez-Aguado for her experimental contribution, to Sonata Valentiniene for technical assistance, and to Drs Bruss Lima, Ralf Galuske, and Sergio Neuenschwander for analysis tools. *Conflict of Interest*: None declared.

References

Antonini A, Berlucchi G, Lepore F. 1983. Physiological organization of callosal connections of a visual lateral suprasylvian cortical area in the cat. J Neurophysiol. 49:902–921.

Berbel P, Innocenti GM. 1988. The development of the corpus callosum in cats: a light- and electron-microscopic study. J Comp Neurol. 276:132–156.

Berlucchi G, Rizzolatti G. 1968. Binocularly driven neurons in visual cortex of split-chiasm cats. Science. 159:308–310.

Blakemore C. 1969. Binocular depth discrimination and the nasotemporal division. J Physiol. 205:471–497.

Blakemore C. 1970. Binocular depth perception and the optic chiasm. Vision Res. 10:43–47.

Blakemore C, Diao YC, Pu ML, Wang YK, Xiao YM. 1983. Possible functions of the interhemispheric connexions between visual cortical areas in the cat. J Physiol. 337:331–349.

Brus-Ramer M, Carmel JB, Martin JH. 2009. Motor cortex bilateral motor representation depends on subcortical and interhemispheric interactions. J Neurosci. 29:6196–6206.

Buhl EH, Singer W. 1989. The callosal projection in cat visual cortex as revealed by a combination of retrograde tracing and intracellular injection. Exp Brain Res. 75:470–476.

Carmeli C, Knyazeva MG, Innocenti GM, De Feo O. 2005. Assessment of EEG synchronization based on state-space analysis. Neuroimage. 25:339–354.

Carmeli C, Lopez-Aguado L, Schmidt KE, De Feo O, Innocenti GM. 2007. A novel interhemispheric interaction: modulation of neuronal cooperativity in the visual areas. PLoS One. 12:e1287.

Choudhury BP, Whitteridge D, Wilson ME. 1965. The function of the callosal connections of the visual cortex. Q J Exp Physiol Cogn Med Sci. 50:214–219.

Cissé Y, Grenier F, Timofeev I, Steriade M. 2003. Electrophysiological properties and input-output organization of callosal neurons in cat association cortex. J Neurophysiol. 89:1402–1413.

Conti F, Manzoni T. 1994. The neurotransmitters and postsynaptic actions of callosally projecting neurons. Behav Brain Res. 64:37–53.

Coppola DM, White LE, Fitzpatrick D, Purves D. 1998. Unequal representation of cardinal and oblique contours in ferret visual cortex. Proc Natl Acad Sci U S A. 95:2621–2623.

Crook JM, Eysel UT. 1992. GABA-induced inactivation of functionally characterized sites in cat visual cortex (area 18): effects on orientation tuning. J Neurosci. 12:1816–1825.

Crook JM, Kisvarday ZF, Eysel UT. 1996. GABA-induced inactivation of functionally characterized sites in cat visual cortex (area 18): effects on direction selectivity. J Neurophysiol. 75:2071–2088.

Dreher B, Cottee LJ. 1975. Visual receptive-field properties of cells in area 18 of cat's cerebral cortex before and after acute lesions in area 17. J Neurophysiol. 38:735–750.

Engel AK, König P, Kreiter AK, Singer W. 1991. Interhemispheric synchronization of oscillatory neuronal responses in cat visual cortex. Science. 252:1177–1179.

Fabri M, Manzoni T. 1996. Glutamate decarboxylase immunoreactivity in corticocortical projecting neurons of rat somatic sensory cortex. Neuroscience. 72:435–448.

Fabri M, Polonara G, Mascioli G, Paggi P, Salvolini U, Manzoni T. 2006. Contribution of the corpus callosum to bilateral representation of the trunk midline in the human brain: an fMRI study of callosotomized patients. Eur J Neurosci. 23:3139–3148.

Gardner JC, Cynader MS. 1987. Mechanisms for binocular depth sensitivity along the vertical meridian of the visual field. Brain Res. 413:60–74.

Girardin CC, Martin KC. 2009. Inactivation of lateral connections in cat area 17. Eur J Neurosci. 29:2092–2102.

Grigonis AM, Rayos del Sol-Padua RB, Murphy EH. 1992. Visual callosal projections in the adult ferret. Vis Neurosci. 9:99–103.

Gross CG, Bender DB, Mishkin M. 1977. Contributions of the corpus callosum and the anterior commissure to visual activation of inferior temporal neurons. Brain Res. 131:227–239.

Guillemot JP, Paradis MC, Samson A, Ptito M, Richer L, Lepore F. 1993. Binocular interaction and disparity coding in area 19 of visual cortex in normal and split-chiasm cats. Exp Brain Res. 94:405–417.

Houzel J-C, Milleret C, Innocenti GM. 1994. Morphology of callosal axons interconnecting areas 17 and 18 of the cat. Eur J Neurosci. 6:898–917.

Hubel DH, Wiesel TN. 1967. Cortical and callosal connections concerned with the vertical meridian of visual fields in the cat. J Neurophysiol. 30:1561–1573.

Hughes CM, Peters A. 1992. Symmetric synapses formed by callosal afferents in rat visual cortex. Brain Res. 583:271–278.

Innocenti GM. 1986. General organization of callosal connections in the cerebral cortex. In: Jones EG, Peters A, editors. Cerebral cortex. Vol. 5. New York: Plenum Publishing Corporation. p. 291–353.

Innocenti GM, Manger PR, Masiello I, Colin I, Tettoni L. 2002. Architecture and callosal connections of visual areas 17, 18, 19 and 21 in the ferret (Mustela putorius). Cereb Cortex. 12:411–422.

Innocenti GM, Manzoni T, Spidalieri G. 1972. Peripheral and transcallosal reactivity of neurones within SI and SII cortical areas. Segmental divisions. Arch Ital Biol. 110:415–443.

Innocenti GM, Manzoni T, Spidalieri G. 1973. Relevance of the callosal transfer in defining the peripheral reactivity of somesthetic cortical neurones. Arch Ital Biol. 111:187–221.

Innocenti GM, Price DJ. 2005. Exuberance in the development of cortical networks. Nat Rev Neurosci. 6:955–965.

Kalberlah C, Distler C, Hoffmann KP. 2009. Sensitivity to relative disparity in early visual cortex of pigmented and albino ferrets. Exp Brain Res. 192:379–389.

Kennedy H, Meissirel C, Dehay C. 1991. Callosal pathways and their compliancy to general rules governing the organization of corticocortical connectivity. In: Dreher B Robinson S. Vision and visual dysfunction, Vol. 3, neuroanatomy of the visual pathways and their development. London: Macmillan. p. 324–359.

Kiper DC, Knyazeva MG, Tettoni L, Innocenti GM. 1999. Visual stimulus-dependent changes in interhemispheric EEG coherence in ferrets. J Neurophysiol. 82:3082–3094.

Kiper DC, Zesiger P, Maeder P, Innocenti GM. 2002. Vision after early-onset lesions of the occipital cortex: i) Neuropsychological and psychophysical studies. Neural Plast. 9:1–25.

Knyazeva MG, Kiper DC, Vildavsky VJ, Despland PA, Maeder-Ingvar M, Innocenti GM. 1999. Visual stimulus-dependent changes in interhemispheric EEG coherence in humans. J Neurophysiol. 82:3095–3107.

LaMantia AS, Rakic P. 1990. Axon overproduction and elimination in the corpus callosum of the developing rhesus monkey. J Neurosci. 10:2156–2175.

Law MI, Zahs KR, Stryker MP. 1988. Organization of primary visual cortex (area 17) in the ferret. J Comp Neurol. 278:157–180.

Lepore F, Guillemot JP. 1982. Visual receptive field properties of cells innervated through the corpus callosum in the cat. Exp Brain Res. 46:413–424.

Li L, Ebner F. 2006. Balancing bilateral sensory activity: callosal processing modulates sensory transmission through the contralateral thalamus by altering response threshold. Exp Brain Res. 172:397–415.

Lomber SG, Payne BR, Horel JA. 1999. The cryoloop: an adaptable reversible cooling deactivation method for behavioral or electrophysiological assessment of neural function. J Neurosci Methods. 86:179–194.

Makarov VA, Schmidt KE, Castellanos NP, Lopez-Aguado L, Innocenti GM. 2008. Stimulus-dependent interaction between the visual areas 17

and 18 of the 2 hemispheres of the ferret (Mustela Putorius). Cereb Cortex. 18:1951–1960.
Mansfield RJ. 1974. Neural basis of orientation perception in primate vision. Science. 186:1133–1135.
Marzi CA, Antonini A, Di Stefano M, Legg CR. 1982. The contribution of the corpus callosum to receptive fields in the lateral suprasylvian visual areas of the cat. Behav Brain Res. 4:155–176.
Mitchell DE, Blakemore C. 1970. Binocular depth perception and the corpus callosum. Vision Res. 10:49–54.
Nakamura H, Chaumon M, Klijn F, Innocenti GM. 2008. Dynamic properties of the representation of the visual field midline in the visual areas 17 and 18 of the ferret (*Mustela putorius*). Cereb Cortex. 18:1941–1950.
Nowak LG, Munk MHJ, Nelson JI, James AC, Bullier J. 1995. Structural basis of cortical synchronization. I. Three types of interhemispheric coupling. J Neurophysiol. 74:2379–2400.
Orban GA, Kennedy H. 1981. The influence of eccentricity on receptive field types and orientation selectivity in areas 17 and 18 of the cat. Brain Res. 208:203–208.
Payne BR. 1994. Neuronal interactions in cat visual cortex mediated by the corpus callosum. Behav Brain Res. 64:55–64.
Payne BR, Berman N. 1983. Functional organization of neurons in cat striate cortex: variations in preferred orientation and orientation selectivity with receptive-field type, ocular dominance, and location in visual-field map. J Neurophysiol. 49:1051–1072.
Payne BR, Elberger AJ, Berman N, Murphy EH. 1980. Binocularity in the cat visual cortex is reduced by sectioning the corpus callosum. Science. 207:1097–1099.
Payne BR, Siwek DF, Lomber SG. 1991. Complex transcallosal interactions in visual cortex. Vis Neurosci. 6:283–289.
Peters A, Payne BR, Josephson K. 1990. Transcallosal non-pyramidal cell projections from visual cortex in the cat. J Comp Neurol. 302: 124–142.
Pettigrew JD, Nikara T, Bishop PO. 1968. Responses to moving slits by single units in cat striate cortex. Exp Brain Res. 6:373–390.
Prince SJD, Pointon AD, Cumming BG, Parker AJ. 2002. Quantitative analysis of the responses of V1 neurons to horizontal disparity in dynamic random-dot stereograms. J Neurophysiol. 87:191–208.
Ptito M. 2003. Functions of the corpus callosum as derived from split-chiasm studies in cats. In: Zaidel E, Iacobini M, editors. The parallel brain: the cognitive neuroscience of the corpus callosum. Cambridge (MA): Massachusetts Institute of Technology Press. p. 139–153.
Rochefort NL, Buzás P, Kisvárday ZF, Eysel UT, Milleret C. 2007. Layout of transcallosal activity in cat visual cortex revealed by optical imaging. Neuroimage. 36:804–821.
Rochefort NL, Buzás P, Quenech'du N, Koza A, Eysel UT, Milleret C, Kisvárday ZF. 2009. Functional selectivity of interhemispheric connections in cat visual cortex. Cereb Cortex. 19:2451–2465.
Schmidt KE, Kim DS, Singer W, Bonhoeffer T, Löwel S. 1997. Functional specificity of long-range intrinsic and interhemispheric connections in the visual cortex of strabismic cats. J Neurosci. 17: 5480–5492.
Schmidt KE, Löwel S. 2002. Long-range intrinsic connections in cat primary visual cortex. In: Peters A, Payne BR, editors. The cat primary visual cortex. San Diego (CA): Academic Press. p. 387–426.
Segraves MA, Innocenti GM. 1985. Comparison of the distributions of ipsilaterally and contralaterally projecting corticocortical neurons in cat visual cortex using two fluorescent tracers. J Neurosci. 5:2107–2118.
Segraves MA, Rosenquist AC. 1982. The afferent and efferent callosal connections of retinotopically defined areas in cat cortex. J Neurosci. 2:1090–1107.
Swindale N. 1998. Orientation tuning curves: empirical description and estimation of parameters. Biol Cybern. 78:45–56.
Tettoni L, Gheorghita-Baechler F, Bressoud R, Welker E, Innocenti GM. 1998. Constant and variable aspects of axonal phenotype in cerebral cortex. Cereb Cortex. 8:543–552.
Toyama K, Matsunami K, Ohno T, Tokashiki S. 1974. An intracellular study of neuronal organization in the visual cortex. Exp Brain Res. 21:45–66.
Wang G, Ding S, Yunokuchi K. 2003. Representation of cardinal contour overlaps less with representation of nearby angles in cat visual cortex. J Neurophysiol. 90:3912–3920.
White LE, Bosking WH, Williams SM, Fitzpatrick D. 1999. Maps of central visual space in ferret V1 and V2 lack matching inputs from the two eyes. J Neurosci. 19:7089–7099.